



Toward a Dinuclear-System Description of Cluster States in Medium-Mass $N \approx Z$ Nuclei

A. Rahmatinejad,
A. Mukhammadsoliev, T. M. Shneidman

Bogoliubov Laboratory of Theoretical Physics
Joint Institute for Nuclear Research, Dubna

October 2026

From dinuclear systems to cluster states

- Cluster resonances have been observed in light and medium-mass nuclei near $N = Z$, including titanium isotopes.
- We investigate a molecular picture in which an α-particle is coupled to a deformed core.
- We developed a framework based on DNS approach to describe the excited states of a molecular system by explicitly treating the coupling between the relative collective motion and the excited states of the core.

Aim

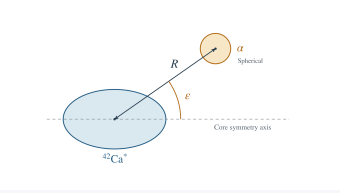
To investigate how the interaction and channel coupling shape collective bands and determine their electromagnetic transition strengths.

- Formulate a multichannel framework for studying cluster resonances.
- Analyze how the interaction, radial motion, and channel coupling determine the structure of collective states.
- Apply the framework to $\alpha + {}^{42}\mathrm{Ca}^{*}$ configurations in ${}^{46}\mathrm{Ti}$.

DNS interaction potential

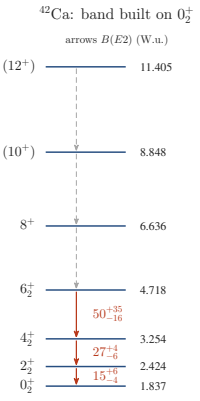
The $\alpha + {}^{42}\mathrm{Ca}^{*}$ configuration

The α particle is spherical, while the excited ${}^{42}\mathrm{Ca}^{*}$ core is axially deformed.



- R: centre-to-centre separation;
- ε: angle between the core symmetry axis and the separation vector.

Axial symmetry removes the dependence on the azimuthal angle.



K. Hadyńska-Klęk et al., PRL 117, 062501 (2016); ENSDF, $A = 42$ evaluation.

- Selected core configuration: the deformed band of ${}^{42}\mathrm{Ca}$ built on 0^{+}_{2} at 1.837 MeV.
- The experimental data support a strongly deformed rotational band with $\beta_2 = 0.43(2)$.
- Here, we approximate this structure by an axial rotor with $\beta_{20} = 0.43$.

$$U_{\mathrm{int}}(R,\varepsilon) = U_{\mathrm{C}}(R,\varepsilon) + U_{\mathrm{N}}(R,\varepsilon).$$

Calculation of the interaction

- **Coulomb interaction:** folding of the fragment proton densities:

$$U_{\mathrm{C}}(R,\varepsilon) = e^2 \iint \frac{\rho_{\alpha}^{(p)}(\mathsf{r}_1)\,\rho_{\mathrm{Ca}}^{(p)}(\mathsf{r}_2)}{|s|}\, d^3 r_1\, d^3 r_2.$$

- **Nuclear interaction:** double folding of the matter densities with the density-dependent effective Migdal interaction:

$$U_{\mathrm{N}}(R,\varepsilon) = \iint \rho_{\alpha}(\mathsf{r}_1)\,\rho_{\mathrm{Ca}}(\mathsf{r}_2)\, v_{\mathrm{NN}}^{\mathrm{Migdal}}(\mathsf{s};\rho_{\alpha},\rho_{\mathrm{Ca}})\, d^3 r_1\, d^3 r_2.$$

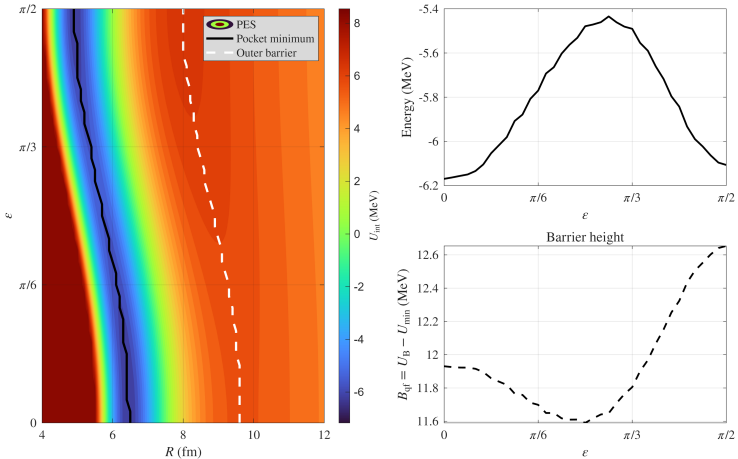
$$\mathsf{s} = \mathsf{R} + \mathsf{r}_1 - \mathsf{r}_2,$$

where r_1 and r_2 are measured from the respective fragment centers.

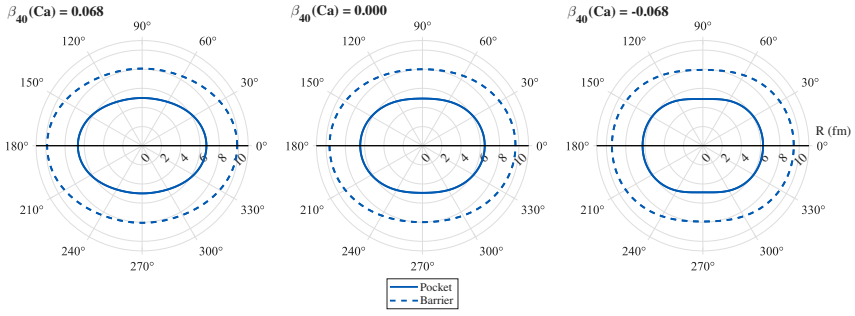
Density distributions: Gaussian for the spherical α particle; deformed Fermi for the core. The core deformation parameters (β_{20}, β_{40}) are fixed inputs for each potential-energy surface.

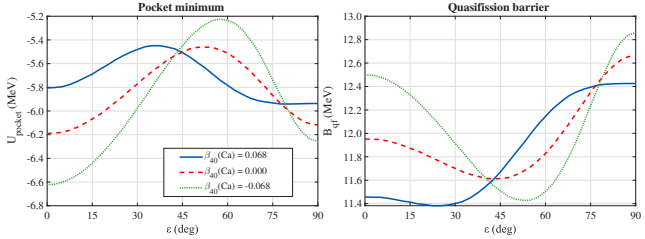
Orientation dependence of the interaction potential

At each ε, the radial potential determines the pocket minimum and the outer barrier. Their positions describe the preferred molecular geometry, and their energy difference gives the quasi-fission barrier: $B_{\mathrm{qf}}(\varepsilon) = U_{\mathrm{int}}(R_{\mathrm{b}}, \varepsilon) - U_{\mathrm{int}}(R_{\mathrm{min}}, \varepsilon)$.



Effect of core deformation on the interaction potential





Core excitations and channel basis

The excited $^{42}\mathrm{Ca}$ core is described by selected states $\Phi_{L_H M_H}$ with excitation energies $E_H(L_H)$. $\longrightarrow$ taken from experimental data.

Angular-momentum coupling

Since the α particle has spin zero,

$$\mathsf{I} = \mathsf{L}_H + \mathsf{L}_R, \qquad |L_H - L_R| \le I \le L_H + L_R.$$

Here L_H is the core angular momentum and L_R is the relative orbital angular momentum. For one selected core band, a channel is labelled by $c = (L_H, L_R)$.

The channel functions are

$$\mathcal{Y}_c^{IM}(\Omega_H, \widehat{\mathsf{R}}) = \Big[\Phi_{L_H}(\Omega_H) \otimes Y_{L_R}(\widehat{\mathsf{R}})\Big]_{IM},$$

and the total wave function is expanded as

$$\Psi^{IM} = \sum_c A_c^I \frac{\chi_c^I(R)}{R}\, \mathcal{Y}_c^{IM}(\Omega_H, \widehat{\mathsf{R}}).$$

From the PES to channel-dependent radial potentials

The interaction matrix in the channel basis is

$$V^{I}_{cc'}(R) = \left\langle \mathcal{Y}^{IM}_{c} \middle| \hat{U}_{\rm int}(R) \middle| \mathcal{Y}^{IM}_{c'} \right\rangle ,$$

where the integration includes the core and relative-motion angular coordinates.

Diagonal-channel potentials

For each channel $c = (L_H, L_R)$, the diagonal potential is an angular average of the calculated PES:

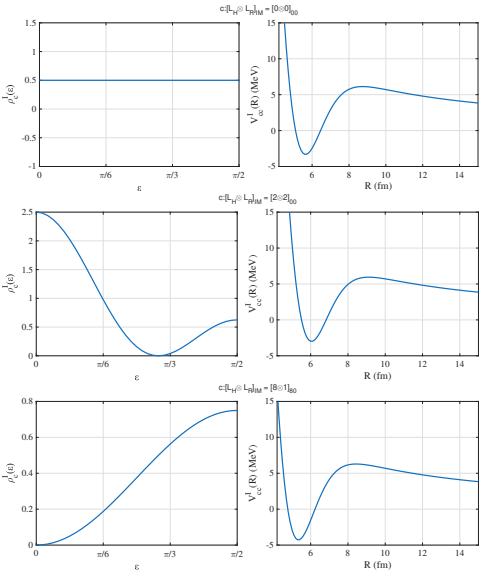
$$V^{I}_{cc}(R) = 2 \int_{0}^{\pi/2} \rho^{I}_{c}(\varepsilon)\, U_{\rm int}(R,\varepsilon)\, \sin\varepsilon \, d\varepsilon .$$

The orientation weight is

$$\rho^{I}_{c}(\varepsilon) = \mathcal{N}_c \frac{2L_H+1}{2I+1} \sum_{K=-\min(I,L_R)}^{\min(I,L_R)} |\langle L_H 0, L_R K \mid IK\rangle|^2 \left| \sqrt{2\pi}\, Y_{L_R K}(\varepsilon, 0) \right|^2 .$$

- Different channels sample different orientations of the same PES.
- Their angular weights determine the resulting radial pocket and barrier.

Examples of channel-dependent potentials



Bound-state approximation for the radial pocket states

- The effective radial potential in channel c is:

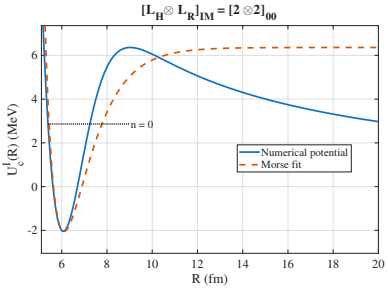
$$U_c^I(R) = V_{cc}^I(R) + \frac{\hbar^2 L_R(L_R+1)}{2\mu R^2}.$$

- The centrifugal contribution is governed by L_R, not I. It raises the effective radial potential and can weaken or remove the pocket at sufficiently large L_R.
- Schrodinger equation for radial potential,

$$\left[-\frac{\hbar^2}{2\mu}\frac{d^2}{dR^2} + U_c^I(R)\right]\chi_{cn}^I(R) = E_{cn}^I \chi_{cn}^I(R).$$

$\Longrightarrow$ Analytical radial energies E_{cn}^I and wave functions for the subsequent channel coupling $\chi_{cn}^I(R)$.

The localized channel basis terminates when centrifugal effects remove the pocket or eliminate the bound Morse state of the selected radial branch.



Morse fit to the radial pocket

$$U_{\mathrm{M}}(R) = U_{\min} + D_e\left[1 - e^{-a(R-R_e)}\right]^2.$$

- R_e: position of the pocket minimum;
- D_e: depth relative to the Morse asymptote;
- a: controls the pocket width and curvature.

Coupling between channels

Using the radial states obtained in each diagonal channel, we expand the total wave function as

$$\Psi_{\nu}^{IM} = \sum_{c,n} A_{cn}^{I\nu} \, \frac{\chi_{cn}^{I}(R)}{R} \, \mathcal{Y}_{c}^{IM}.$$

Effective Hamiltonian in the radial-channel basis

$$H_{cn,c'n'}^{I} = \left[E_H(L_H) + E_{cn}^{I} + S_\alpha\right] \delta_{cc'}\delta_{nn'} + (1-\delta_{cc'}) \int \chi_{cn}^{I*}(R)\, V_{cc'}^{I}(R)\, \chi_{c'n'}^{I}(R)\, dR.$$

The diagonal term includes the core excitation energy and the radial energy. The off-diagonal terms couple different channels.

The energies and mixing amplitudes follow from diagonalization:

$$\sum_{c',n'} H_{cn,c'n'}^{I} \, A_{c'n'}^{I\nu} = E_{\nu}^{I} \, A_{cn}^{I\nu}.$$

- Mixing occurs between channels with the same total angular momentum and parity.
- The weights $|A_{cn}^{I\nu}|^2$ characterize the composition of each calculated state.
- $S_\alpha = 8.006$ MeV.

Examples of channel mixing

State	E_ν (MeV)	Leading wave-function components ($I = 0$)
1	11.18	$0.84[0 \otimes 0]^+_0 + 0.54[2 \otimes 2]^+_0 + \cdots$
2	13.40	$0.73[2 \otimes 2]^+_0 - 0.50[0 \otimes 0]^+_0 + 0.46[4 \otimes 4]^+_0 + \cdots$
3	16.26	$0.84[4 \otimes 4]^+_0 - 0.42[2 \otimes 2]^+_0 + 0.26[6 \otimes 6]^+_0 + \cdots$
4	20.61	$0.95[6 \otimes 6]^+_0 - 0.26[4 \otimes 4]^+_0 + \cdots$
5	26.14	$0.98[8 \otimes 8]^+_0 + \cdots$

State	E_ν (MeV)	Leading wave-function components ($I = 4$)
1	12.70	$0.76[2 \otimes 2]^+_4 + 0.61[4 \otimes 0]^+_4 + \cdots$
2	12.79	$0.97[4 \otimes 1]^-_4 + 0.15[6 \otimes 3]^-_4 + \cdots$
3	13.19	$0.68[4 \otimes 0]^+_4 - 0.52[2 \otimes 2]^+_4 - 0.32[0 \otimes 4]^+_4 + 0.30[6 \otimes 2]^+_4 + 0.22[2 \otimes 4]^+_4 + \cdots$
4	13.69	$0.94[2 \otimes 3]^-_4 - 0.23[4 \otimes 3]^-_4 - 0.16[2 \otimes 5]^-_4 + \cdots$
5	14.35	$0.79[4 \otimes 2]^+_4 + 0.46[0 \otimes 4]^+_4 - 0.21[4 \otimes 4]^+_4 + 0.18[4 \otimes 0]^+_4 + 0.17[6 \otimes 4]^+_4 + \cdots$

Channel mixing varies strongly between states.

Electromagnetic transitions

The reduced transition probabilities are calculated using the coupled-channel wave functions:

$$B(E\lambda; I_i \to I_f) = \frac{1}{2I_i + 1} \left| \left\langle \Psi_f^{I_f} \left\| \hat{\mathcal{M}}(E\lambda) \right\| \Psi_i^{I_i} \right\rangle \right|^2 .$$

- $E2$ **transitions:** contributions from the intrinsic core excitation and relative motion.
- $E1$ **transitions:** generated by relative motion between the clusters in the present model.
- $E2$ transitions preserve parity, whereas $E1$ transitions connect states of opposite parity.
- Different N/Z ratios of the α particle and core allow relative-motion $E1$ transitions between opposite-parity states.

Transition strengths provide information on the collective structure of the calculated states.

Identification of rotational bands

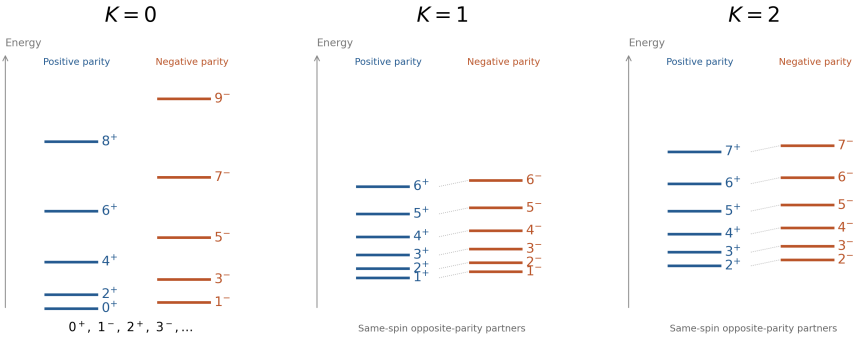
The calculated $B(E2)$ values are used to identify collective sequences.

1. Select the lowest-energy unassigned state as a candidate bandhead.
2. Follow the strongest available $\Delta I = 2$ $E2$ transitions.
3. Repeat the procedure to identify additional bands.

$$I_{\mathrm{bh}} \xleftarrow{E2} I_{\mathrm{bh}} + 2 \xleftarrow{E2} I_{\mathrm{bh}} + 4 \xleftarrow{E2} \cdots$$

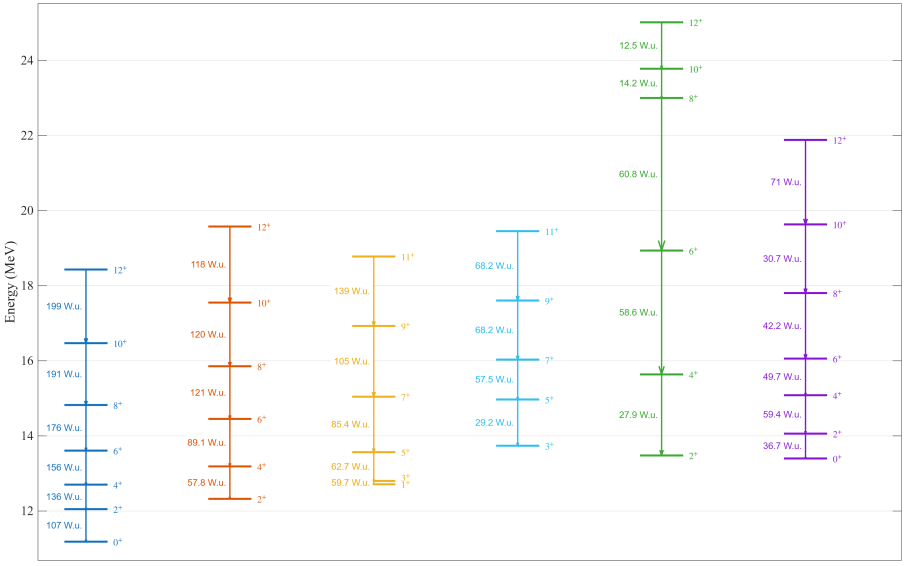
Electromagnetic transitions allow us to identify candidate collective bands.

Conventional K-band

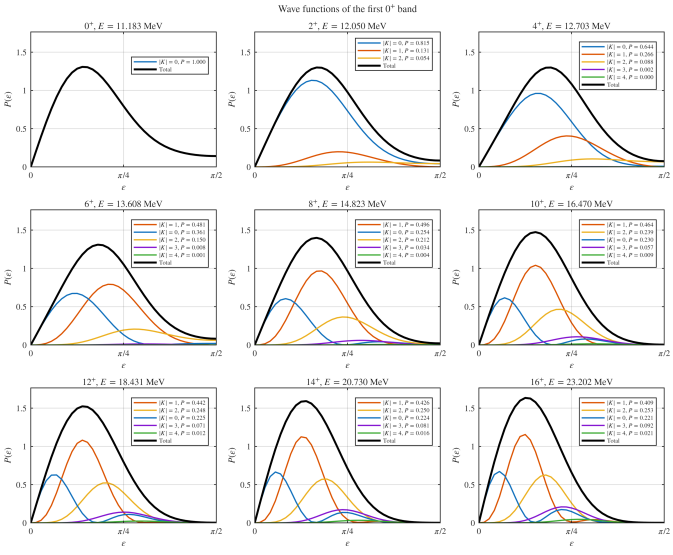


$K = 0$: usual alternating-parity family. $K > 0$: illustrative parity-partner bands with $I \gtrsim K$.

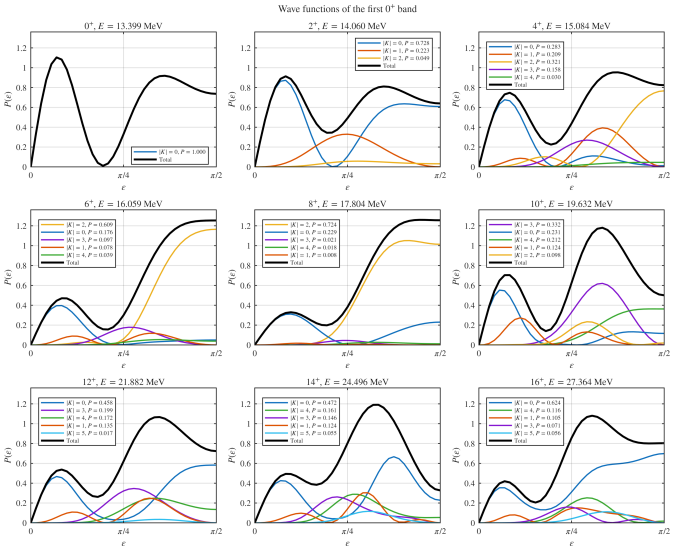
Calculated positive-parity bands in ^{46}Ti: ^{42}Ca* + α



Angular distribution of the wave functions: first 0^+ band



Angular distribution of the wave functions: second 0^+ band



The internal orientation distribution is state dependent.

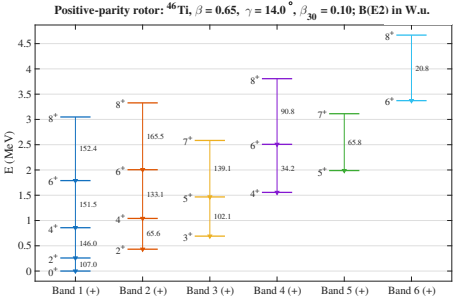
Rigid versus dynamical nonaxiality

Rigid triaxial rotor

- Fixed nonaxial intrinsic geometry.
- Three principal moments of inertia.
- Rotational motion can produce mixing of K components.

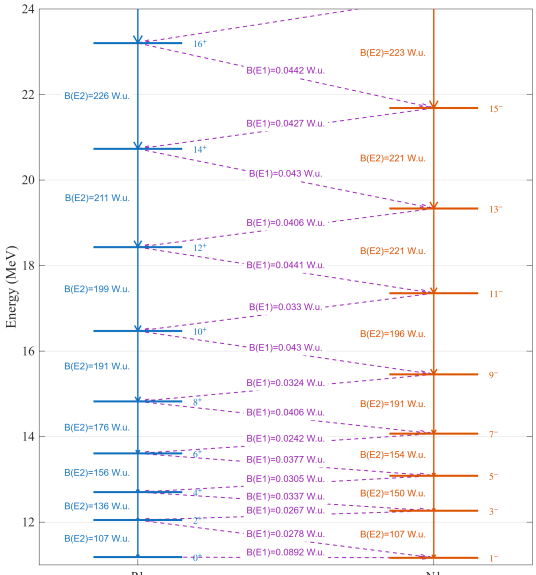
Dinuclear system

- Axially deformed core coupled to an α-particle.
- Relative orientation is a dynamical coordinate.
- Angular distributions and K mixing depend on the state.

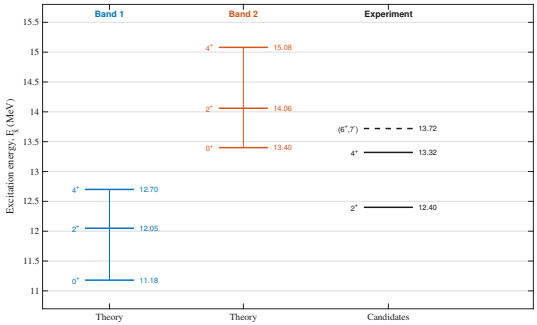


Rotational bands do not necessarily imply a rigid triaxial intrinsic shape.

Positive- and negative-parity bands with interband E1 transitions



^{46}Ti: comparison of molecular bands with experimental α-cluster candidates



Expt. data: Fukada et al., Phys. Rev. C 80, 064613 (2009).

- Absolute excitation energies are sensitive to the details of the DNS interaction potential.
- The experimental level spacing is closer to that of the second calculated 0^+ band.

Relative level spacings may provide a more robust criterion for identifying molecular configurations.

Conclusions

- A coupled-channel DNS framework has been developed for describing $\alpha + {}^{42}\mathrm{Ca}^{*}$ cluster configurations in ${}^{46}\mathrm{Ti}$.
- The calculated $E2$ transitions identify collective band candidates with different degrees of channel mixing. The angular distributions reveal state-dependent orientation dynamics, without assuming a rigid triaxial shape.
- Positive- and negative-parity states emerge naturally from the relative orbital motion. The model predicts $E1$ transitions connecting opposite-parity bands.

Thank you for your attention!

Electromagnetic transitions

The calculated coupled-channel states determine the reduced transition probabilities:

$$B(E\lambda; I_i\nu_i \to I_f\nu_f) = \frac{1}{2I_i+1}\left|\left\langle \Psi^{I_f}_{\nu_f}\right\| \hat{\mathcal{M}}(E\lambda) \left\|\Psi^{I_i}_{\nu_i}\right\rangle\right|^2.$$

Contributions to the transition operator

$$\hat{\mathcal{M}}(E\lambda) = \hat{\mathcal{M}}_{\rm core}(E\lambda) + \hat{\mathcal{M}}_{\rm rel}(E\lambda).$$

The transition matrix elements include the channel amplitudes, radial overlaps, and angular-momentum coupling. Contributions from different channels are added coherently.

- $B(E2)$: transitions between states of the same parity; identification of collective bands.
- $B(E1)$: transitions between states of opposite parity; connections between positive- and negative-parity sequences.

Electric transition operators

Quadrupole transitions

$$\hat{\mathcal{M}}_{2\mu}(E2) = \hat{\mathcal{M}}^{H}_{2\mu}(E2) + eZ^{(2)}_{\mathrm{rel}} R^2 Y_{2\mu}(\widehat{R}),$$

$$Z^{(2)}_{\mathrm{rel}} = Z_\alpha \left(\frac{A_H}{A}\right)^2 + Z_H \left(\frac{A_\alpha}{A}\right)^2.$$

The core quadrupole moment and the relative motion both contribute to the transition amplitude.

Dipole transitions

$$\hat{\mathcal{M}}_{1\mu}(E1) = eZ^{(1)}_{\mathrm{rel}} R Y_{1\mu}(\widehat{R}), \qquad Z^{(1)}_{\mathrm{rel}} = \frac{Z_\alpha A_H - Z_H A_\alpha}{A}.$$

The relative dipole moment reflects the difference between the charge-to-mass ratios of the two fragments.

Matrix elements are evaluated between the coupled-channel wave functions, retaining interference between their components.